

ISSN 2063-5346



SIGNIFICANCE OF SHAPE FACTOR AND DIFFERENT HEAT SOURCES AND ON A WATER BASED HYBRID NANOFLUID FLOW OVER A SHRINKING SHEET WITH VARIABLE VISCOSITY

Potlapula Usharani^{1*}, B. Ravindra Reddy²

Article History: Received: 10.05.2023

Revised: 29.05.2023

Accepted: 09.06.2023

Abstract

Objective of this study is to examine the influence of the variable viscosity, thermal radiation and exponential heat source parameters on a hybrid nanofluid (Water + Multi-Walled Carbon Nanotubes (*MWCNT*) + Copper (II) oxide (*CuO*)) flow over a shrinking sheet with suction. Governing equations, which are partial differential equations, are converted into the system of nonlinear ordinary differential equations by using appropriate similarity transformations and this system has been solved using the *bvp4c* solver. The heat transmission rate and friction factor against the pertinent parameters are explained using bar graphs. It is observed that, at $0 \leq \phi_{MWCNT} \leq 0.09$, (the volume fraction of *MWCNT*) the skin friction coefficient increases at a rate of 7.828962 (in case of Platelet) and 7.826693 (in case of Cylinder). It is noticed that the rise in magnetic field parameter (Mg) and exponential heat source (Q_e) decrease the Nusselt number. It is noticed that, when $0.1 \leq Q_e \leq 0.7$, the heat transfer rate (Nusselt number) is found to decrease by 0.43786 (in case of Platelet) and 0.43137 (in case of Cylinder). It has been found that when the magnetic field parameter upsurges, the velocity declines. Furthermore, it is detected that the increase in thermal radiation enhances the fluid temperature.

Keywords: Thermal radiation, Hybrid nanofluid, Shrinking sheet, Exponential heat source, Suction.

¹Research Scholar, Department of Mathematics, JNTUH-Hyderabad, Kukatpally – 500085, India. Usharani471981@gmail.com

²Professor, Department of Mathematics, JNTUH-Hyderabad, Kukatpally – 500085, India. rbollareddy@gmail.com

DOI:10.48047/ecb/2023.12.9.45

Nomenclature

σ	Electrical conductivity	η	Similarity variable
Pr	Prandtl number	σ^*	Stefan-Boltzmann constant
k^*	Mean absorption coefficient	Mg	Magnetic field Parameter
ν	Kinematic viscosity	u, v	Components of velocity in two (x, y) directions
k	Thermal conductivity	Ra	Thermal radiation parameter
ϕ_{MWCNT}	Volume fraction of multi-walled carbon nanotube	q_e	Coefficient of Exponential Space related heat Source
ϕ_{CuO}	Volume fraction of Copper (II) Oxide	q_t	Coefficient of Thermal dependent heat Source
g	Acceleration due to gravity	S	Mass transfer parameter where $S > 0$ indicates suction and $S < 0$ indicates injection
λ	Mixed convection parameter	κ, a	Constants and $a > 0$ for liquids
C_p	Specific heat capacity		
v_w	Mass flux velocity		
δ	Temperature dependent fluid viscosity parameter		
β_T	Thermal expansion coefficient		

1 Introduction

Recent years have seen a number of studies that examine the effects of changing the thermo-physical characteristics of the working fluid on the transmission of heat. Due to its improved thermal conductivity and convective coefficient of heat transmission in contrast to the base fluid, nanofluid has been employed in numerous real engineering sectors, including the energy supply, photonics, and electronics industries (M'hamed et al. [1]). Singh et al. [2] studied the thermal conductivity and viscosity properties of a commercial SiC-water nanofluid. Thermal conductivity is observed to rise with particle loadings and to be greater than the expectations of effective medium theory (EMT) for noninteracting spheres. The steady boundary layer flow of a nanofluid through a moving semi-infinite flat plate was theoretically investigated by Bachok et al. [3]. Dual solutions are seen to exist when

the plate and the free stream flow are moving in different directions. Das et al. [4] used the Runge-Kutta-Fehlberg technique to investigate the magnetic field and solar radiation's effects on the nanofluid's slippery flow on a stretching surface. The thickness of the thermal boundary layer is found to grow proportionally with the slip velocity. The flow of a magnetic nanofluid over a stretched plate subjected to thermal radiation was studied quantitatively by Sheikholeslami et al. [5]. The results show that an increase in magnetic parameter causes a thinning of the hydraulic boundary layer. The boundary layer flow of a nanofluid over a variable viscosity wedge was studied by Das et al. [6]. The skin friction coefficient is found to increase as the Brownian motion parameter rises. Rasool et al. [7] discussed a MHD Darcy-Forchheimer nanofluid flow over a nonlinear stretching sheet with Brownian motion and thermophoresis parameters.

Using a Riga plate emitting nonlinear thermal radiation, Abdul Hakeem et al. [8] examined various nanofluid flows. As can be seen, the temperature ratio parameter helps to improve the temperature distribution. Basha and Sivaraj [9] numerically analysed the transport characteristics of blood based nanofluid flow over the plate and wedge towards a stagnation point. Later, different scholars [10 – 12] described various nanofluid flows via distinct geometries. When compared to mono fluids, the heat transmission properties of hybrid fluids are superior. These are finding uses in an extensive diversity of fields, from solar energy to air conditioning. Under a constant heat flux boundary condition, Suresh et al. [13] studied the laminar heat transfer and frictional properties of a water-based hybrid nanofluid with a 0.1% volume concentration as it passed through a straight circular tube. Compared to pure water, the experimental findings of using a hybrid nanofluid for laminar flow indicated a maximum improvement in Nusselt number of 13.56 percent at a Reynolds number of 1730. Labib et al. [14] discussed the hydrodynamic and thermal behaviour of laminar forced convection flow nanofluids inside the uniformly heated tube. Three-dimensional rotating flow of water-based hybrid nanofluid across a stretched surface with thermal radiation, heat generation, and chemical reaction was investigated by Hayat and Nadeem [15]. In the presence of a Cattaneo-Christov heat flux model, Jamshed and Aziz [16] conducted a computational analysis of heat transfer and entropy generation for boundary layer flow of conventional and hybrid Casson nanofluids. The fluid flow and heat transmission characteristics of a water-based hybrid nanofluid flow through a stretching cylinder subjected to Joule

heating and viscous dissipation were studied by Maskeen et al. [17]. It has been shown that the presence of hybrid material increases the convective heat transfer, which is at its lowest in the case of copper/water nanofluid. Several studies [18 - 22] then discussed various hybrid nanofluid flows over different geometries.

In view of the preceding research, nobody has up until now tried to explain the significance of variable viscosity and shape factor effects, for the radiative hybrid nanofluid (Water + *MWCNT* + *CuO*) flow with exponential heat source. Engineering parameters of concern including friction factor are explained using bar graphs.

2 Mathematical Formulation

A laminar and steady radiative hybrid nanofluid flow (Water + *MWCNT* + *CuO*) flow with variable viscosity and exponential heat source is considered in this study and flat plate is assumed as a geometry. Thermophysical characteristics of water (base fluid), *MWCNT* and *CuO* (nanoparticles) are shown in Table 1. Following are the assumptions for the current study:

- (i) x – axis is taken as along the plate (parallel to the flow), while the y – axis will be transverse to it, as shown in Fig. 1.
- (ii) There is a magnetic field employed in the direction of y – axis, with a strength of B_0 .
- (iii) The shrinking velocity of the sheet is $u_w = -ax$ with $a > 0$ being shrinking constant.
- (iv) Joule heating, induced magnetic field and viscous dissipation are neglected.

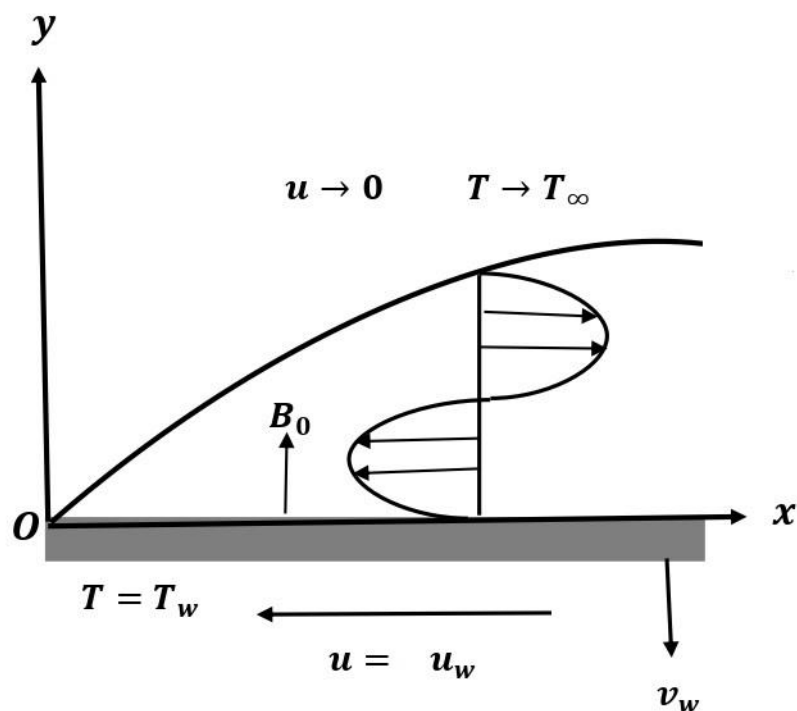


Fig. 1 Schematic diagram

These assumptions lead to the following governing equations and boundary conditions (Al-Kouz et al. [23]):

$$\frac{\partial u}{\partial x} + \frac{\partial v}{\partial y} = 0 \quad (1)$$

$$u \frac{\partial u}{\partial x} + v \frac{\partial u}{\partial y} = \frac{1}{\rho_{hnf}} \frac{\partial}{\partial y} \left(\mu_{hnf} \frac{\partial u}{\partial y} \right) + g \beta_T (T - T_\infty) - \frac{\sigma_{hnf}}{\rho_{hnf}} B_0^2 u \quad (2)$$

$$\left(\rho C_p \right)_{hnf} \left(u \frac{\partial T}{\partial x} + v \frac{\partial T}{\partial y} \right) = k_{hnf} \frac{\partial^2 T}{\partial y^2} + \frac{16\sigma^* T_\infty^3}{3k^*} \frac{\partial^2 T}{\partial y^2} + q_e (T_w - T_\infty) \exp \left(-my \sqrt{\frac{a}{\nu}} \right) \quad (3)$$

$$+ q_t (T - T_\infty)$$

$$\left. \begin{array}{l} \text{at } y = 0 : u = u_w, v = v_w, T = T_w, \\ \text{as } y \rightarrow \infty : u \rightarrow 0, T \rightarrow T_\infty. \end{array} \right\} \quad (4)$$

2.1 Hybrid nanofluid (HNF) thermophysical characteristics

$$\left. \begin{aligned} (\rho C_p)_{hnf} &= \left[(1 - \phi_{MWCNT})(\rho C_p)_f + \phi_{MWCNT}(\rho C_p)_{MWCNT} \right] (1 - \phi_{CuO}) + (\rho C_p)_{CuO} \phi_{CuO}, \\ \sigma_{nf} &= \frac{\sigma_{MWCNT} + 2\sigma_f - 2\sigma_f \phi_{MWCNT} + 2\sigma_{MWCNT} \phi_{MWCNT}}{\sigma_{MWCNT} + 2\sigma_f + \sigma_f \phi_{MWCNT} - \sigma_{MWCNT} \phi_{MWCNT}} \times \sigma_f, \\ \rho_{hnf} &= \left[(1 - \phi_{MWCNT})\rho_f + \phi_{MWCNT}\rho_{MWCNT} \right] (1 - \phi_{CuO}) + \rho_{CuO}\phi_{CuO}, \\ \mu_{hnf} &= \frac{\mu_f}{(1 - \phi_{MWCNT})^{2.5} (1 - \phi_{CuO})^{2.5}}, \\ \sigma_{hnf} &= \frac{\sigma_{CuO} + 2\sigma_{nf} - 2\sigma_{nf} \phi_{CuO} + 2\sigma_{CuO} \phi_{CuO}}{\sigma_{CuO} + 2\sigma_{nf} + \sigma_{nf} \phi_{CuO} - \sigma_{CuO} \phi_{CuO}} \times \sigma_{nf}. \end{aligned} \right\}$$

and

$$k_{hnf} = \frac{k_{CuO} + (n+1)k_{nf} - (n+1)k_{nf} \phi_{CuO} + (n+1)k_{CuO} \phi_{CuO}}{k_{CuO} + (n+1)k_{nf} + k_{nf} \phi_{CuO} - k_{CuO} \phi_{CuO}} \times k_{nf},$$

$$k_{nf} = \frac{k_{MWCNT} + (n+1)k_f - (n+1)k_f \phi_{MWCNT} + (n+1)k_{MWCNT} \phi_{MWCNT}}{k_{MWCNT} + (n+1)k_f + k_f \phi_{MWCNT} - k_{MWCNT} \phi_{MWCNT}} \times k_f.$$

(Sheikholeslami and Rokni [24])

The shape parameter is denoted by n here. Several shapes of nanoparticles are represented in Table 1 with their corresponding shape factors.

Note that the variable viscosity coefficient μ_f is defined as (Nadeem et al. [25]):

$$\frac{1}{\mu_f} = \frac{1}{\mu_{f\infty}} [1 + \kappa(T - T_v)] \quad \text{or} \quad \frac{1}{\mu_f} = a(T - T_v)$$

where $a = \frac{\kappa}{\mu_{f\infty}}$ and $T_v = T_\infty - \frac{1}{\kappa}$.

Table 1 Nanoparticle forms and values of their respective shape factors (Sheikholeslami and Rokni [24])



S. No.		Name of the shape	n
1		Platelet	5.7
2		Cylinder	4.8

Table 2 Thermophysical property values for base fluid and nanomaterials (Alzahrani et al. [26])

S. No.		H_2O (f)	$MWCNT$ (ϕ_{MWCNT})	CuO (ϕ_{CuO})
1	$\rho(kgm^{-3})$	997.1	2100	6320
2	$k(W(m K)^{-1})$	0.613	3000	76.5
3	$C_p(J(kg K)^{-1})$	4179	711	531.8
4	$\sigma(Sm^{-1})$	0.0000055	0.00019	2.7×10^{-8}

Das et al. [27] recommended the succeeding similarity variables to alter controlling equations:

$$u = \alpha x f'(\eta), v = -\sqrt{av} f, \eta = y \sqrt{\frac{u_w}{\nu x}}, \theta(\eta) = \frac{T - T_\infty}{T_w - T_\infty} \quad (5)$$

(5)

Then (5) makes (1) to fulfil and redraft (2–4) as:

$$\frac{1}{A_1 A_2} \frac{\delta}{\delta - \theta} f''' + f f'' - f'^2 + \frac{1}{A_1 A_2} \frac{\delta}{(\delta - \theta)^2} f'' \theta' + \lambda \theta - \frac{A_3 Mg}{A_1} f' = 0 \quad (6)$$

(6)

$$\frac{A_4}{A_5} \frac{1}{Pr} \theta'' + \frac{1}{A_5} \frac{Ra}{Pr} \theta'' + f \theta' + \frac{Q_e}{A_5} \exp(-m\eta) + \frac{Q_t}{A_5} \theta = 0 \quad (7)$$

$$\left. \begin{aligned} \text{at } \eta = 0: f(\eta) = S, f'(\eta) = -1, \theta(\eta) = 1 \\ \text{at } \eta \rightarrow \infty: f'(\eta) \rightarrow 0, \theta(\eta) \rightarrow 0 \end{aligned} \right\} \quad (8)$$

where

$$\left. \begin{aligned} \delta = -\frac{1}{\kappa(T_w - T_\infty)}, Mg = \frac{\sigma B_0^2}{\rho a}, Pr = \frac{\mu C_p}{k}, Ra = \frac{16\sigma^* T_\infty^3}{3kk^*}, \\ \lambda = \frac{Gr}{Re_x^2}, Gr = \frac{g\beta_T(T_w - T_\infty)x^3}{\nu^2}, Re_x = \frac{xu_w}{\nu}, Q_e = \frac{q_e}{a(\rho C_p)}, \\ Q_t = \frac{q_t}{a(\rho C_p)}, S = -\frac{v_w}{\sqrt{av}} \end{aligned} \right\}$$

and

$$\left. \begin{aligned}
 A_2 &= (1 - \phi_{MWCNT})^{2.5} (1 - \phi_{CuO})^{2.5}, \\
 A_5 &= (1 - \phi_{CuO}) \left[(1 - \phi_{MWCNT}) + \phi_{MWCNT} \frac{(\rho C_p)_{MWCNT}}{(\rho C_p)_f} \right] + \phi_2 \frac{(\rho C_p)_{CuO}}{(\rho C_p)_f}, \\
 A_{31} &= \frac{\sigma_{MWCNT} + 2\sigma_f - 2\phi_{MWCNT} (\sigma_f - \sigma_{MWCNT})}{\sigma_{MWCNT} + 2\sigma_f + \phi_{MWCNT} (\sigma_f - \sigma_{MWCNT})}, \\
 A_1 &= (1 - \phi_{CuO}) \left[(1 - \phi_{MWCNT}) + \phi_{MWCNT} \frac{\rho_{MWCNT}}{\rho_f} \right] + \phi_{CuO} \frac{\rho_{CuO}}{\rho_f}, \\
 A_3 &= \frac{\sigma_{CuO} + 2A_{31}\sigma_f - 2\phi_{CuO} (A_{31}\sigma_f - \sigma_{CuO})}{\sigma_{CuO} + 2A_{31}\sigma_f + \phi_{CuO} (A_{31}\sigma_f - \sigma_{CuO})} A_{31}, A_4 = \frac{k_{CuO} + 2A_{41}k_f - 2\phi_{CuO} (A_{41}k_f - k_{CuO})}{k_{CuO} + 2A_{41}k_f + \phi_{CuO} (A_{41}k_f - k_{CuO})} A_{41}, \\
 A_{41} &= \frac{k_{MWCNT} + 2k_f - 2\phi_{MWCNT} (k_f - k_{MWCNT})}{k_{MWCNT} + 2k_f + \phi_{MWCNT} (k_f - k_{MWCNT})}.
 \end{aligned} \right\}$$

Coefficient of skin friction coefficient (C_{fx}) is outlined as:

$$Cf = \frac{\tau_w}{\rho_f u_w^2} \Big|_{y=0}, \tag{9}$$

where $\tau_w = \mu_{mf} \left(\frac{\partial u}{\partial y} \right)$.

Rewriting the expression in (9) with (5) yields

$$\sqrt{Re_x} Cf = \frac{1}{A_2} f''(0).$$

The following formula can be used to calculate the Nusselt number:

$$Nu_x = - \frac{xq_w}{k_f (T_w - T_\infty)} \Big|_{y=0}, \tag{10}$$

where $q_w = \left(k_{mf} + \frac{16\sigma * T_\infty^3}{3k*} \right) \frac{\partial T}{\partial y}$.

The formula in (10) is reworked with the help of (5) as:

$$\sqrt{\frac{1}{Re_x}} Nu_x = -A_4 (1 + Ra) \theta'(0).$$

3 Discussion of outcomes

In order to solve equations (6 - 7) with the conditions (8), the built-in function `bvp4c` of MATLAB is employed.

3.1 Profiles of Engineering Parameters of Concern

According to Figs. 2 - 3, it has been noted that the rise in Mg and ϕ_{MWCNT} enhance the skin friction coefficient. It is observed that, at $0 \leq \phi_{MWCNT} \leq 0.09$, the skin friction coefficient

increases at a rate of 7.828962 (in case of Platelet)) and 7.826693 (in case of Cylinder). It is noticed from Figs. 4 – 5 that the rise in Mg and Q_e decrease the Nusselt number. It is noticed that, when $0.1 \leq Q_e \leq 0.7$, the heat transfer rate (Nusselt number) is found to decrease by 0.43786 (in case of Platelet) and 0.43137 (in case of Cylinder).

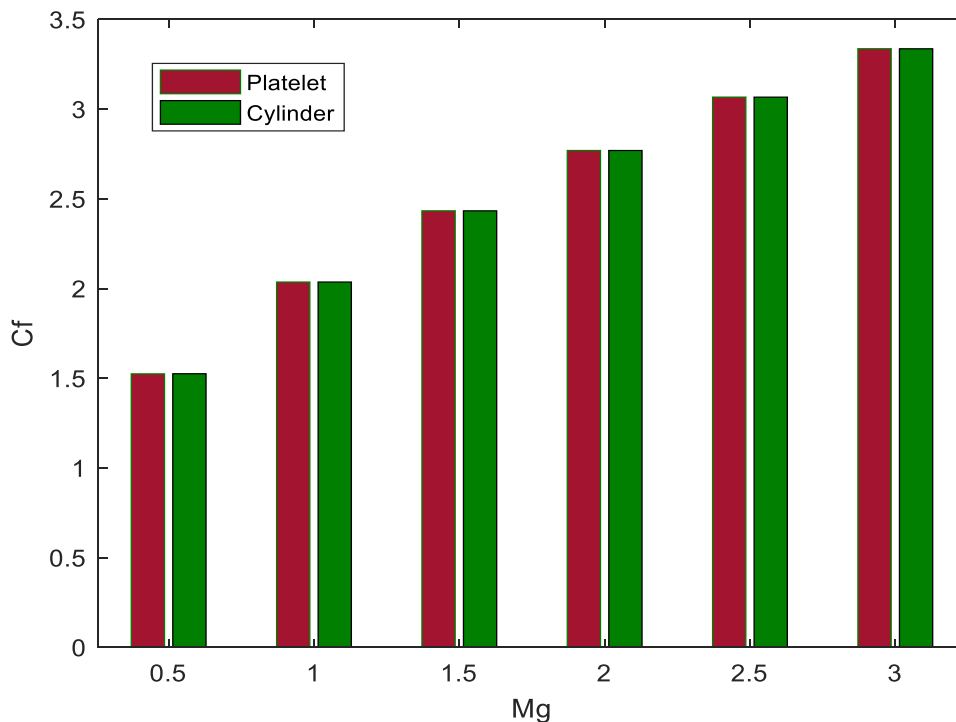


Fig. 2 Profile of skin friction coefficient with the impact of Mg

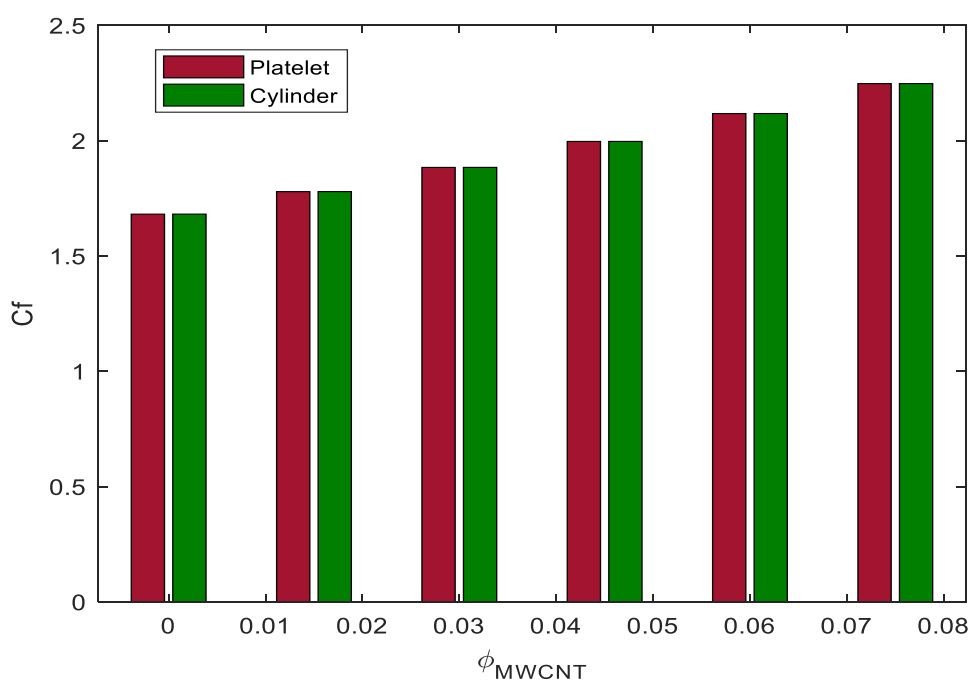


Fig. 3 Profile of skin friction coefficient profile with the impact of ϕ_{MWCNT}

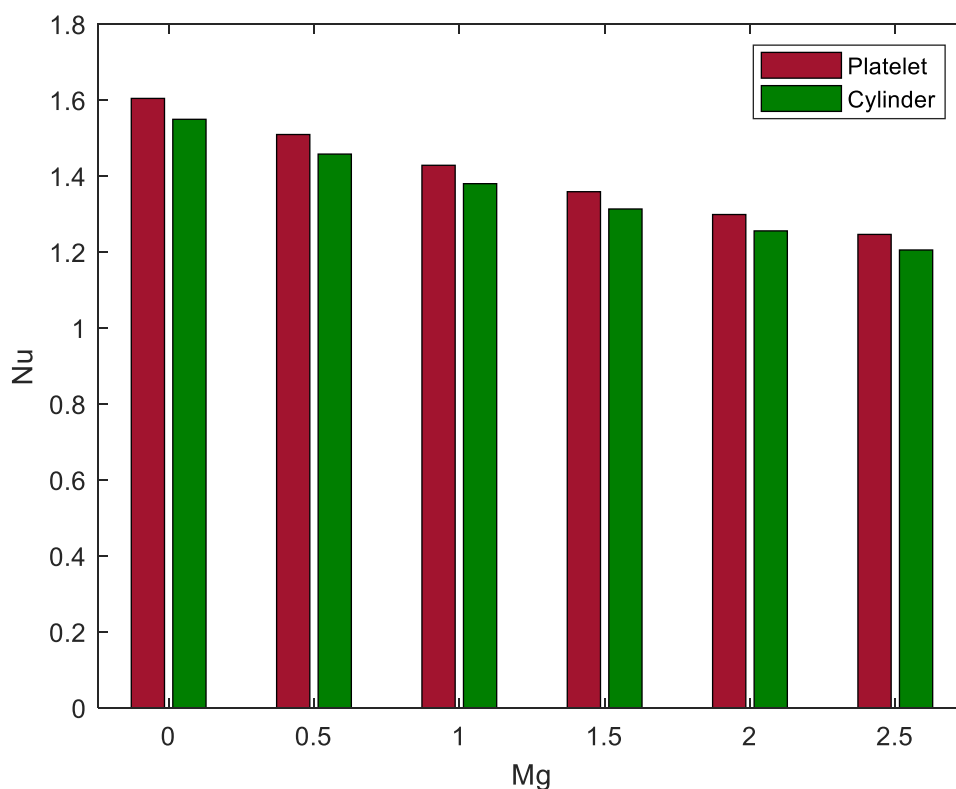


Fig. 4 Profile of Nusselt number with the impact of Mg

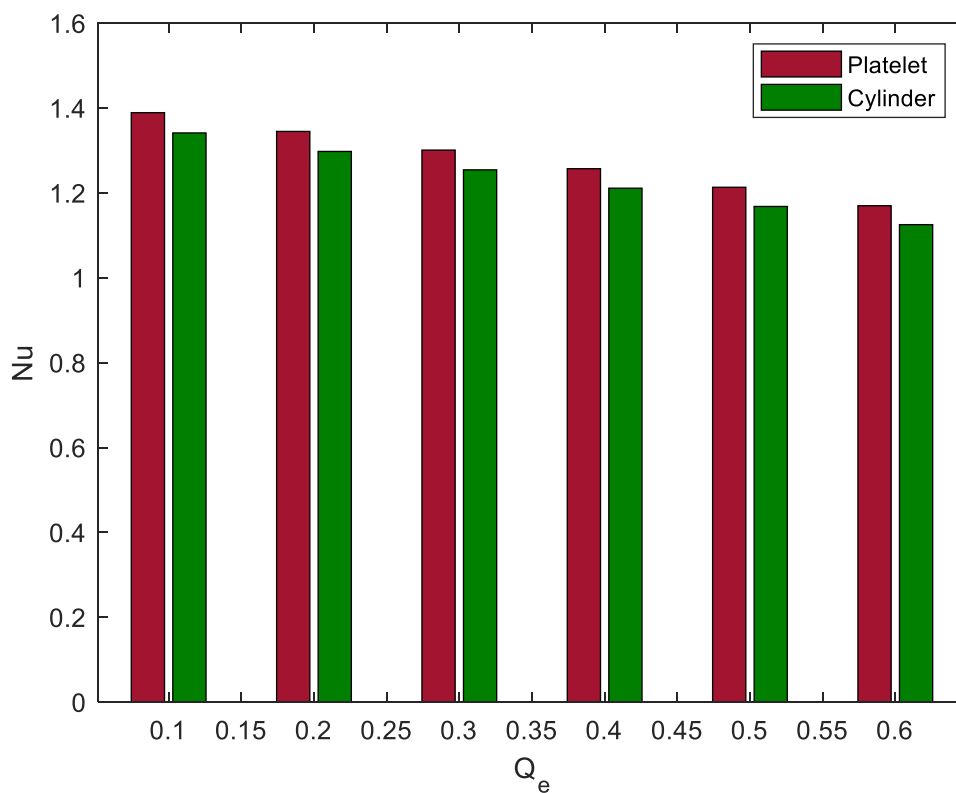


Fig. 5 Profile of Nusselt number with the impact of Q_e

3.2 Temperature and Velocity Profiles

As a result of the thermal radiation parameter, heat is transferred to the fluid. There will be a greater transfer of heat energy from the source to the fluid if this value is made larger. Therefore, as seen in Fig. 6, the temperature rises as the fluid particles absorb heat energy. From Fig. 7, it is clear that the rise in Q_e enhances the fluid temperature. It is because of the extra heat supplied to the liquid system by the ESHS (Heat Source related to Exponential space) mechanism. Fig. 8 exhibits the fact that the fluid temperature enriches with the upsurge in Q_i . In Fig. 9, we can see that when

ϕ_{MWCNT} increases, the fluid's temperature increases. It has been found, as shown in Fig. 10, that when the magnetic field parameter upsurges, the velocity declines. Magnetic flow lines travelled normally through the fluid when an external magnetic field was applied around it. Particles' movement from one layer to another is impeded as a result of the Lorentz force that is created. Due to this, the fluid's molecules travel very slowly. The fluid's velocity slows as a result. According to the Fig. 11, it has been established that an increase in δ results in a decrease in velocity.

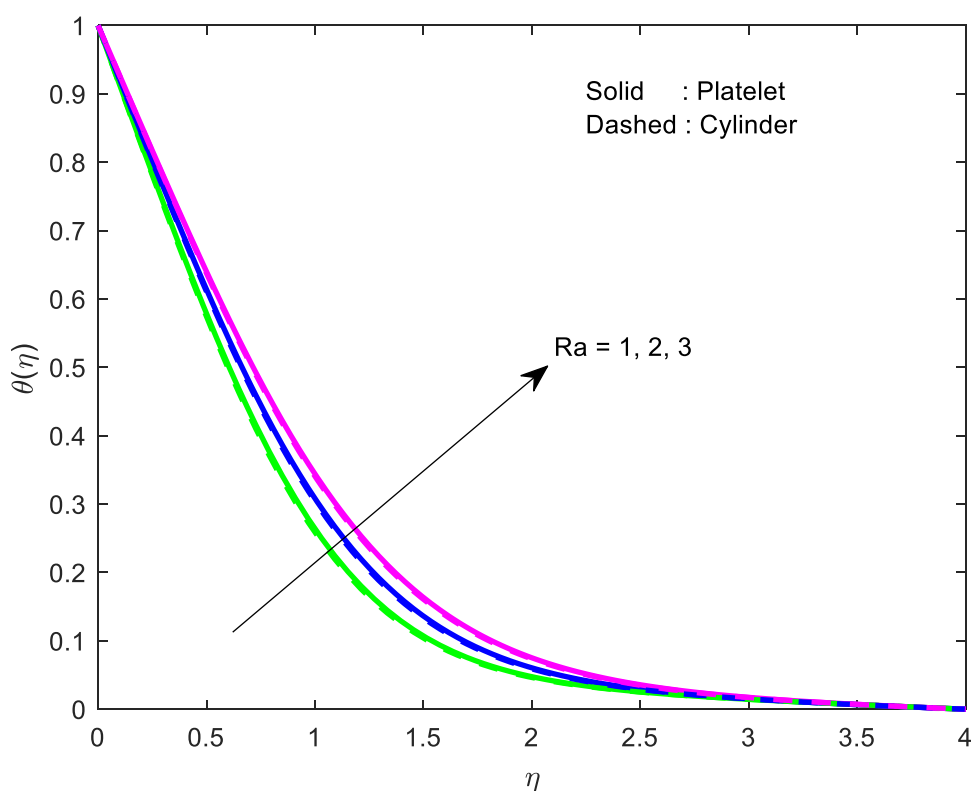


Fig. 6 Profile of $\theta(\eta)$ with the impact of Ra

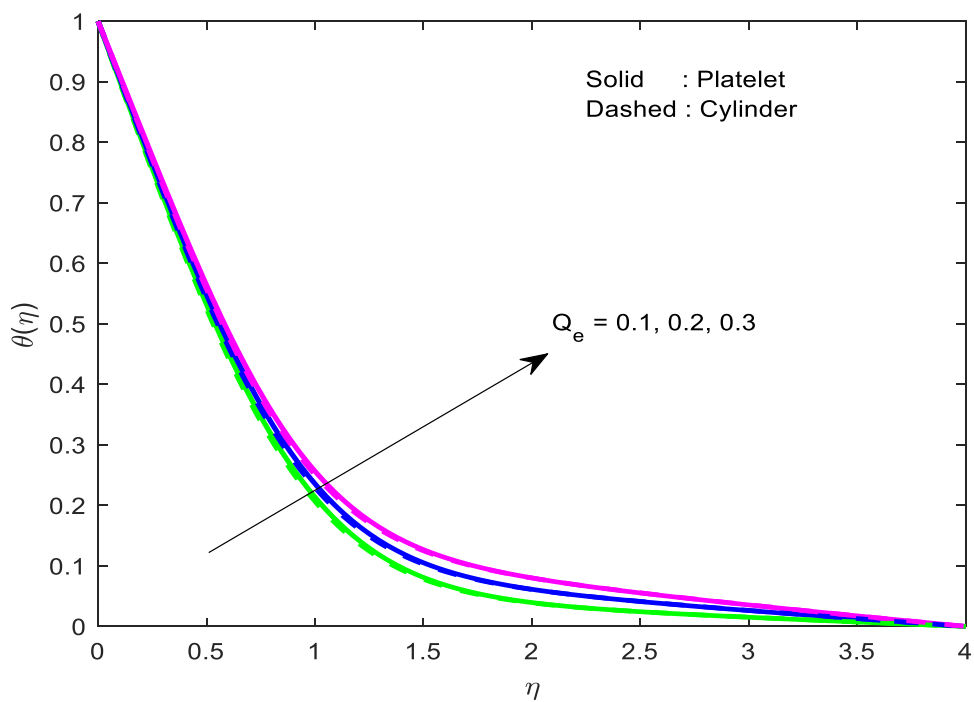


Fig. 7 Profile of $\theta(\eta)$ with the impact of Q_e

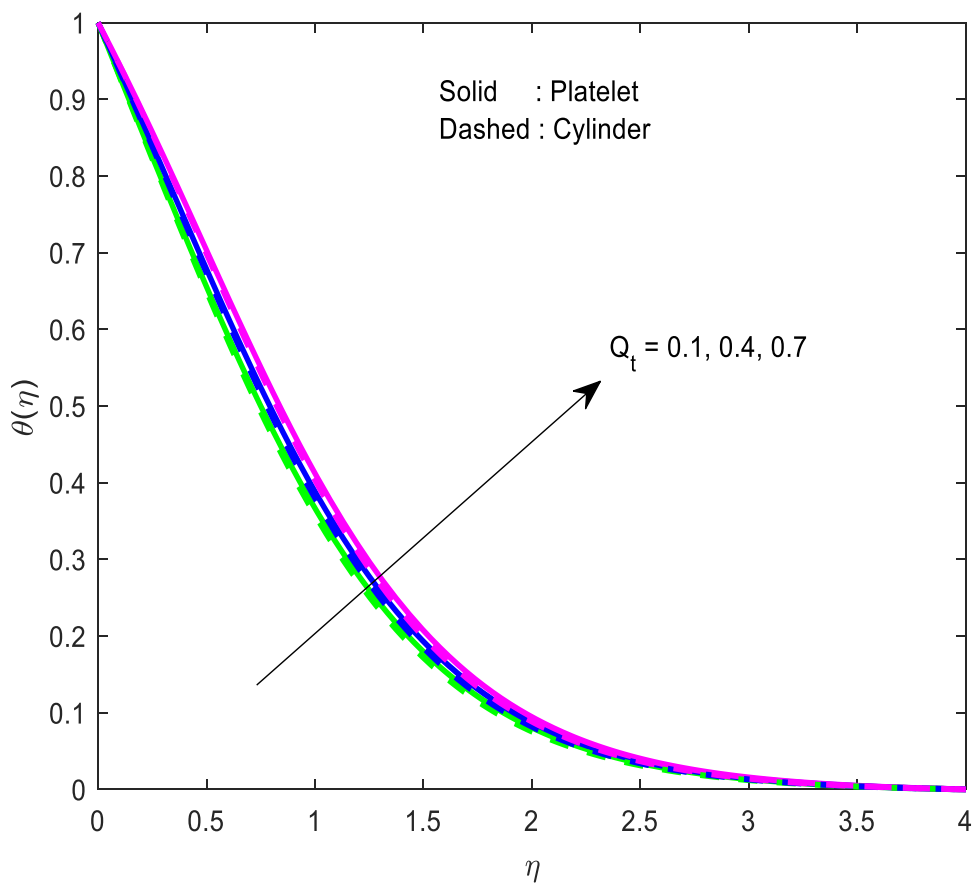


Fig. 8 Profile of $\theta(\eta)$ with the impact of Q_t

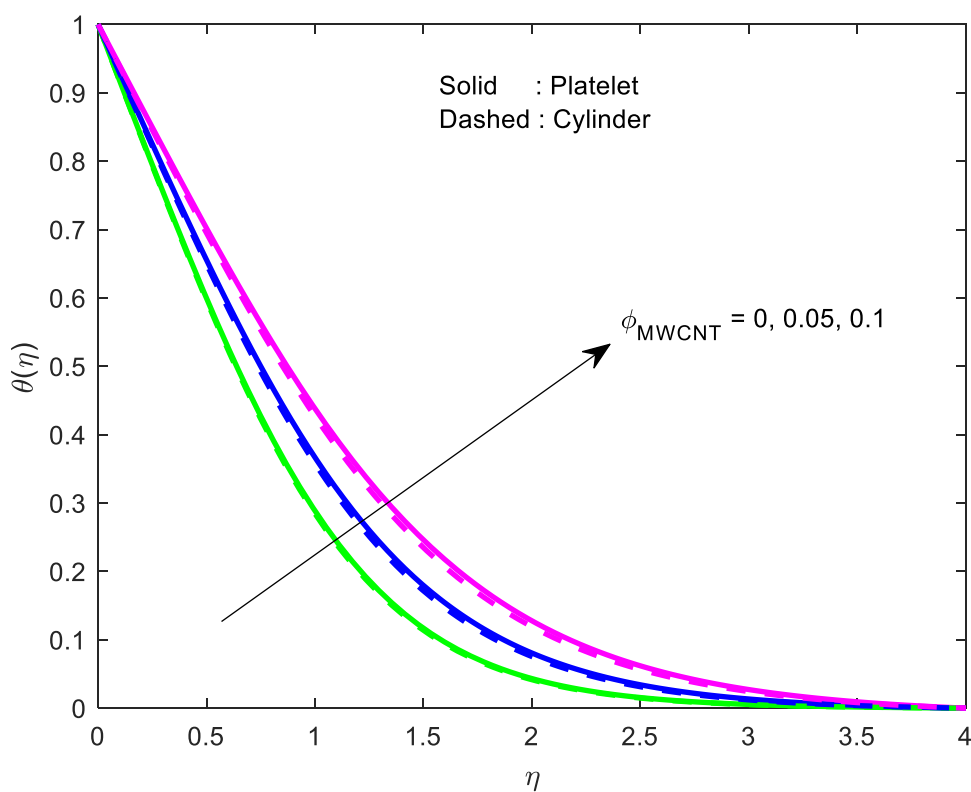


Fig. 9 Profile of $\theta(\eta)$ with the impact of ϕ_{MWCNT}

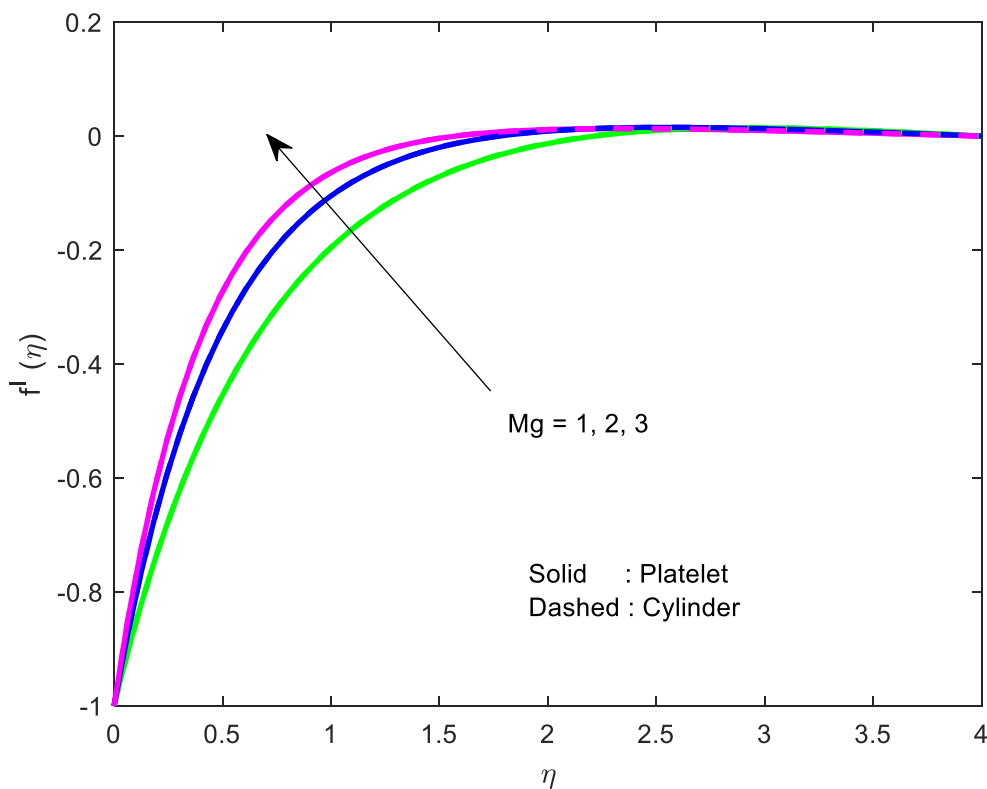


Fig. 10 Profile of $f'(\eta)$ with the impact of Mg

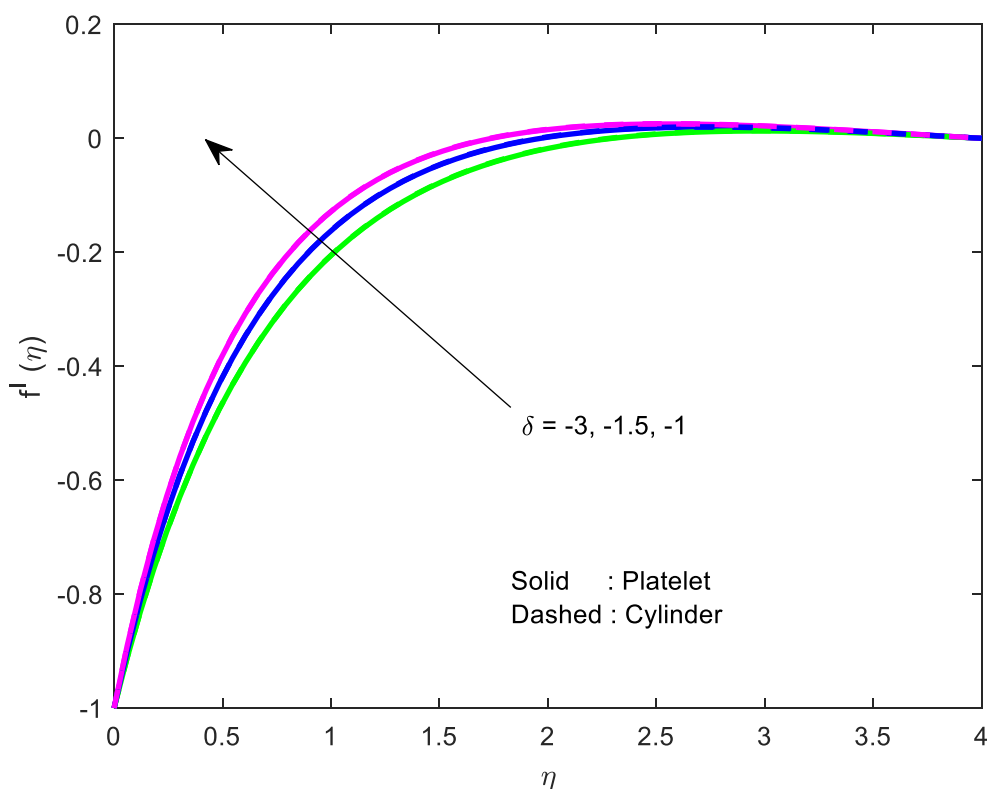


Fig. 11 Profile of $f'(\eta)$ with the impact of δ

4 Conclusions

Objective of this paper is how thermal radiation and variable viscosity parameters effect the characteristics of hybrid nanofluid (Water + $MWCNT$ + CuO) flow over a shrinking sheet with different heat source parameters. The study's findings are briefly summarised below.

- It is observed that, at $0 \leq \phi_{MWCNT} \leq 0.09$, (the volume fraction of $MWCNT$) the skin friction coefficient increases at a rate of 7.828962 (in case of Platelet)) and 7.826693 (in case of Cylinder).
- It is noticed that the rise in magnetic field parameter (Mg) and exponential heat source (Q_e) decrease the Nusselt number.
- It is noticed that, when $0.1 \leq Q_e \leq 0.7$, the heat transfer rate (Nusselt number) is found to

decrease by 0.43786 (in case of Platelet) and 0.43137 (in case of Cylinder).

- It has been found that when the magnetic field parameter upsurges, the velocity declines.
- It is detected that the increase in thermal radiation enhances the fluid temperature.

References

1. M'hamed B, Sidik NA, Yazid MN, Mamat R, Najafi G, Kefayati GH. A review on why researchers apply external magnetic field on nanofluids. *International Communications in Heat and Mass Transfer*. 2016;78:60-67.
2. Singh D, Timofeeva E, Yu W, Routbort J, France D, Smith D, Lopez-Cepero JM. An investigation of silicon carbide-water nanofluid

- for heat transfer applications. *Journal of Applied Physics*. 2009;105(6):064306.
3. Bachok N, Ishak A, Pop I. Boundary-layer flow of nanofluids over a moving surface in a flowing fluid. *International Journal of Thermal Sciences*. 2010;49(9):1663-1668.
 4. Das K, Duari PR, Kundu PK. Solar radiation effects on Cu–water nanofluid flow over a stretching sheet with surface slip and temperature jump. *Arabian Journal for Science and Engineering*. 2014;39:9015-9023.
 5. Sheikholeslami M, Mustafa MT, Ganji DD. Effect of Lorentz forces on forced-convection nanofluid flow over a stretched surface. *Particuology*. 2016;26:108-113.
 6. Das K, Acharya N, Kundu PK. Influence of variable fluid properties on nanofluid flow over a wedge with surface slip. *Arabian Journal for Science and Engineering*. 2018;43:2119-2131.
 7. Rasool G, Shafiq A, Khalique CM, Zhang T. Magnetohydrodynamic Darcy–Forchheimer nanofluid flow over a nonlinear stretching sheet. *Physica Scripta*. 2019;94(10):105221.
 8. Abdul Hakeem AK, Ragupathi P, Saranya S, Ganga B. Three dimensional non-linear radiative nanofluid flow over a Riga plate. *Journal of Applied and Computational Mechanics*. 2020;6(4):1012-1029.
 9. Basha HT, Sivaraj R. Numerical simulation of blood nanofluid flow over three different geometries by means of gyrotactic microorganisms: applications to the flow in a circulatory system. *Proceedings of the Institution of Mechanical Engineers, Part C: Journal of Mechanical Engineering Science*. 2021;235(2):441-460.
 10. Naveen Kumar R, Suresh Goud J, Srilatha P, Manjunatha PT, Rani SP, Kumar R, Suresha S. Cattaneo–Christov heat flux model for nanofluid flow over a curved stretching sheet: An application of Stefan blowing. *Heat Transfer*. 2022;51(6):4977-4991.
 11. Rawat SK, Yaseen M, Khan U, Kumar M, Abdulrahman A, Eldin SM, Elattar S, Abed AM, Galal AM. Insight into the significance of nanoparticle aggregation and non-uniform heat source/sink on titania–ethylene glycol nanofluid flow over a wedge. *Arabian Journal of Chemistry*. 2023;16(7):104809.
 12. Rasool G, Wakif A, Wang X, Shafiq A, Chamkha AJ. Numerical passive control of alumina nanoparticles in purely aquatic medium featuring EMHD driven non-Darcian nanofluid flow over convective Riga surface. *Alexandria Engineering Journal*. 2023;68:747-762.
 13. Suresh S, Venkitaraj KP, Selvakumar P, Chandrasekar M. Effect of Al₂O₃–Cu/water hybrid nanofluid in heat transfer. *Experimental Thermal and Fluid Science* 2012;38:54-60.
 14. Labib MN, Nine MJ, Afrianto H, Chung H, Jeong H. Numerical investigation on effect of base fluids and hybrid nanofluid in forced convective heat transfer. *International Journal of Thermal Sciences*. 2013;71:163-171.
 15. Hayat T, Nadeem S. Heat transfer enhancement with Ag–CuO/water hybrid nanofluid. *Results in physics*. 2017;7:2317-2324.
 16. Jamshed W, Aziz A. Cattaneo–Christov based study of TiO₂–CuO/EG Casson hybrid nanofluid flow over a stretching surface with entropy generation. *Applied Nanoscience*. 2018;8(4):685-698.

17. Maskeen MM, Zeeshan A, Mehmood OU, Hassan M. Heat transfer enhancement in hydromagnetic alumina–copper/water hybrid nanofluid flow over a stretching cylinder. *Journal of Thermal Analysis and Calorimetry*. 2019;138:1127-1136.
18. Salman S, Talib AA, Saadon S, Sultan MH. Hybrid nanofluid flow and heat transfer over backward and forward steps: A review. *Powder Technology*. 2020;363:448-472.
19. Abbas N, Nadeem S, Saleem A, Malik MY, Issakhov A, Alharbi FM. Models base study of inclined MHD of hybrid nanofluid flow over nonlinear stretching cylinder. *Chinese Journal of Physics*. 2021;69:109-117.
20. Kumar RN, Gowda RP, Abusorrah AM, Mahrous YM, Abu-Hamdeh NH, Issakhov A, Rahimi-Gorji M, Prasannakumara BC. Impact of magnetic dipole on ferromagnetic hybrid nanofluid flow over a stretching cylinder. *Physica Scripta*. 2021;96(4):045215.
21. Lavanya B, Kumar JG, Babu MJ, Raju CS, Shah NA, Junsawang P. Irreversibility Analysis in the Ethylene Glycol Based Hybrid Nanofluid Flow amongst Expanding/Contracting Walls When Quadratic Thermal Radiation and Arrhenius Activation Energy Are Significant. *Mathematics*. 2022;10(16):2984.
22. Mahmood Z, Khan U, Saleem S, Rafique K, Eldin SM. Numerical analysis of ternary hybrid nanofluid flow over a stagnation region of stretching/shrinking curved surface with suction and lorentz force. *Journal of Magnetism and Magnetic Materials*. 2023;573:170654.
23. Al-Kouz W, Mahanthesh B, Alqarni MS, Thriveni K. A study of quadratic thermal radiation and quadratic convection on viscoelastic material flow with two different heat source modulations. *International Communications in Heat and Mass Transfer*. 2021;126:105364.
24. Nadeem S, Ahmed Z, Saleem S. Carbon nanotubes effects in magneto nanofluid flow over a curved stretching surface with variable viscosity. *Microsystem Technologies*. 2019;25:2881-2888.
25. Sheikholeslami M, Rokni HB. Magnetic nanofluid natural convection in the presence of thermal radiation considering variable viscosity. *The European Physical Journal Plus*. 2017;132:238.
26. Alzahrani AK, Ullah MZ, Alshomrani AS, Gul T. Hybrid nanofluid flow in a Darcy-Forchheimer permeable medium over a flat plate due to solar radiation. *Case Studies in Thermal Engineering*. 2021;26:100955.
27. Das K. Nanofluid flow over a shrinking sheet with surface slip. *Microfluidics and nanofluidics*. 2014;16:391-401.